

Real-time Needle Tip Localization in 2D Ultrasound Images for Robotic Biopsies

Mert Kaya*, Enes Senel†, Awais Ahmad*, Orcun Orhan‡, Ozkan Bebek‡,

*Department of Electrical and Electronics Engineering, Ozyegin University, Istanbul, Turkey

Email: mert.kaya@ozyegin.edu.tr, awais.ahmad@ozu.edu.tr

†Department of Computer Science, Ozyegin University, Istanbul, Turkey

Email: enes.senel@ozu.edu.tr

‡Department of Mechanical Engineering, Ozyegin University, Istanbul, Turkey

Email: sabriorcun.orhan@ozyegin.edu.tr, ozkan.bebek@ozyegin.edu.tr

Abstract—In this paper, real-time needle tip tracking method using 2D ultrasound (US) images for robotic biopsies is presented. In this method, the needle tip is estimated with the Gabor filter based image processing algorithm, and the estimation noise is reduced with the Kalman filter. This paper also presents the needle tip tracking simulation to test accuracy of the Kalman filter under position misalignments and tissue deformations. In order to execute proposed method in real-time, the bin packing method is used and the processing time is reduced by 56%, without a GPU. The proposed method was tested in four different phantoms and water medium. The accuracy of the needle tip estimation was measured with optical tracking system, and root mean square error (RMS) of the tip position is found to be 1.17 mm. The experiments showed that the algorithm could track the needle tip in real-time.

I. INTRODUCTION

Percutaneous needle biopsy is a frequently performed medical operation. Precision of the needle insertion plays a significant role in the success of the operation. Particularly during manual insertions, if the needle is placed inaccurately, the tissue sample might be collected from an inaccurate location. A number of repeated misplacements might also cause internal bleeding. In order to improve the placement accuracy, the trajectory of the needle has to be determined correctly and the needle tip should be tracked.

Percutaneous needle procedures are commonly performed using medical imaging. Among other options, ultrasound (US) imaging does not have any known side affects and provides larger workspace. However, the image quality is poor and the US images contain artifacts, which makes the visibility of the needle especially its tip low. In manual insertions planning the trajectory of the needle requires experience and it is not always accurate. Robotic assisted needle insertion is a reliable and accurate way to perform these operations [1], where the robot can move with high resolution, plan the trajectory precisely, and also provide visual feedback for guidance.

This paper presents needle tip tracking in 2D US images using Gabor filter. The needle is inserted using a robotic device, and the needle's tip is tracked using 2D US imaging. In order to perform the method in real time, the bin packing method is used. Also, in order to test the system with imaging

faults and tissue deformations, needle tip tracking simulations are performed.

II. RELATED WORKS IN LITERATURE

In literature, many studies were conducted on biopsy robots and needle localization in US images. Vrooijink et al. [2] developed a robotic system to track the needle tip in three dimensions with 2D ultrasound images. The needle was inserted by a motorized device, the ultrasound probe was servoed by positioning the device and the robotic system provided feedback for image guidance. The specific pattern of the needle in the US lateral section, known as the comet tail artifact (CTA), was used to detect the needle tip. After thresholding and morphological operations, the CTA pattern was detected and the needle tip was localized. Novotny et al. [3] developed a 3D US guided robotic system to track the surgical instrument and localize the target. Passive markers were used to find the instrument tip and the rotation. Radon transform was used to identify passive markers in 3D US images. The robot was controlled with a PD controller and GPU was used to track the instrument in real time. The validation of the system was carried out in a water tank.

Chatelain et al. [4] proposed a method to detect and track manually inserted needle in real time using a 3D US probe mounted on a 6 DOF robotic arm. The needle insertion was detected with geometric median and volume intensity differences. After insertion was detected, prospective needle pixels were obtained with volume intensity differences and the needle axis was localized using RANSAC. The Kalman filter was applied to track the needle more accurately. Mathiassen et al. [5] used second order derivative of 2D Gaussian function and the frame difference data of the sequential frames to estimate the needle tip in 2D US images. The accuracy of the system was measured using an optical tracker.

Ayvaci et al. [6] tracked the biopsy needle in 2D transrectal US images. The needle pixels in the image were mapped using prior knowledge of the needle's position, image background model, and US probe stability. Ding et al. [7] proposed an automatic needle localization algorithm for US guided breast operations. The needle pixels were filtered using the variance mapping method. User defined thresholding was used to binarize the filtered image and then principal component analysis

(PCA) was used to localize the needle axis and its tip. Cao et al. [8] proposed automated catheter detection in 3D images. A likelihood map was generated according to the physical model of catheter. The map was projected onto a single image plane with respect to maximum intensity approach to detect the catheter faster. Renfrew et al. [9] proposed a probabilistic method for active localization of the needles and targets. Their method was based on the maximizing data for the needle and target states. Particle filter was used to estimate states. The method was validated with a simulation study.

Fronheiser et al. [10] and Adebar et al. [11] localized the needle tip using 3D color doppler US device. The needle was vibrated at a high frequency using a piezoelectric buzzer. The RF and color doppler filters were used to detect the tip of needle from 3D US images.

This paper extends the work presented in [12] and [13] by implementing real time needle tip tracking in 2D US images. In our previous studies, the needle axis localization and needle tip estimation in 2D US images were proposed, where the needle axis is localized using a Gabor filter. In this study, the needle tip is also tracked using 2D US imaging, and additionally, the needle tip estimation noise is smoothed using a Kalman filter. The processing time of the proposed localization method is reduced by approximately 56% using the bin packing method, so that the algorithm can be executed in real time. Also, the needle tip tracking simulation is presented to test the Kalman filter performance under image misalignment and tissue deformations.

III. 2D US IMAGE PROCESSING

In the US image guided robotic biopsies, the needle is tracked to be led to the target. As mentioned above, the US images contain artifacts and noise. Therefore, images are processed to segment the needle. The localization method used in this paper was first introduced in [13], which is briefly explained below.

The localization algorithm consists of two similar processing stages (Fig. 1). The needle trajectory and its insertion angle are estimated in the first stage; and the needle tip position is estimated in the second stage. In both stages a Gabor filter is used to segment the needle pixels. Filtered images are automatically binarized using the entropy based parameter tuning method.

In the first stage, a Gabor filter kernel is created according to the reference insertion angle value. After the input image is convolved using the filter kernel, 7×7 a median filter is applied to smooth the filtered image. The smoothed image is then binarized using a multiplication of the tuning parameter (α) and Otsu's threshold value. Next, a morphological erosion by a 3×3 line-shaped structuring element is applied. Finally, the needle trajectory and its insertion angle are estimated using RANSAC line fitting and the needle region of interest (ROI) is created.

In the second stage, a Gabor filter kernel is created using the insertion angle estimated in the first stage because visibility of the needle, especially its tip, reaches to a maximum at the insertion angle. Then, the input image is convolved using the filter kernel and a 7×7 median filter is applied to smoothen

the filtered image. The smoothed image is then binarized using the means of the Otsu's and the tuned threshold values. In the next step, the needle ROI is cropped from the binarized image and probability of each pixel association to the needle tip is calculated. The pixel with the maximum probability is determined as the needle tip, and also the needle tip estimation noise is smoothed using a Kalman filter (Fig. 2).

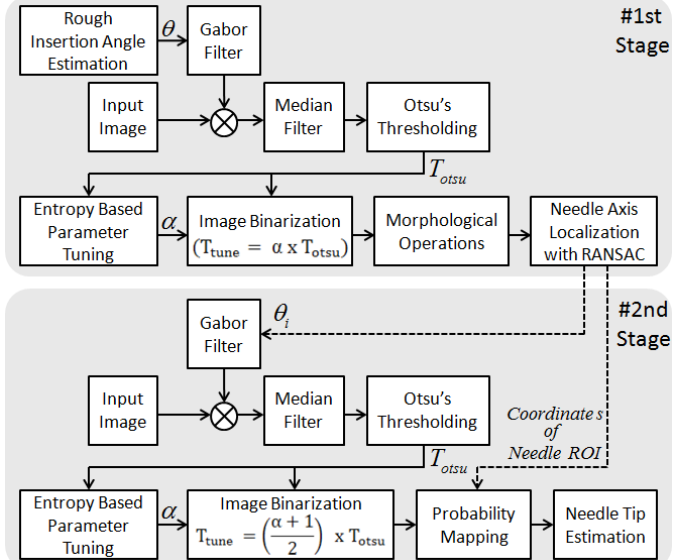


Fig. 1: Flowchart of the proposed needle localization algorithm.

Kalman filter for smoothing the estimation noise: The geometrical shape of the needle is very close to a straight line in 2D US images. In real time, there can be fluctuations in the estimated needle tip trajectory because of the estimation noise coming from the algorithm explained above. The estimation noise originates from varying needle tip visibility and the alignment errors formed between the US probe's imaging plane and the needle.

In 2D US images, the visibility of the tip of the needle can be low, or the tip might be seen as an independent structure from the needle. In these situations, the needle tip is detected with an estimation error. However, if there is a misalignment, the estimation noise can be high. The point where the needle intersects the US image plane is estimated as the needle tip during misalignment occurrences. Also, the needle can disappear completely, or the needle cannot be detected by the RANSAC in the image. As a result, the needle tip cannot be estimated. A Kalman filter is used to smoothen the estimation noise and estimate the position of the needle tip when the needle axis is not detected. The 2D position (x, y) and linear velocities (\dot{x}, \dot{y}) of the target are chosen as states for the Kalman Filter and it is described by

$$x_t = [x \ y \ \dot{x} \ \dot{y}]^T$$

Using the states, dynamic model of the system x_k and the measurement model z_k can be formed as:

$$\begin{aligned} x_k &= Ax_{k-1} + w_k, \\ z_k &= Hx_k + v_k, \end{aligned}$$

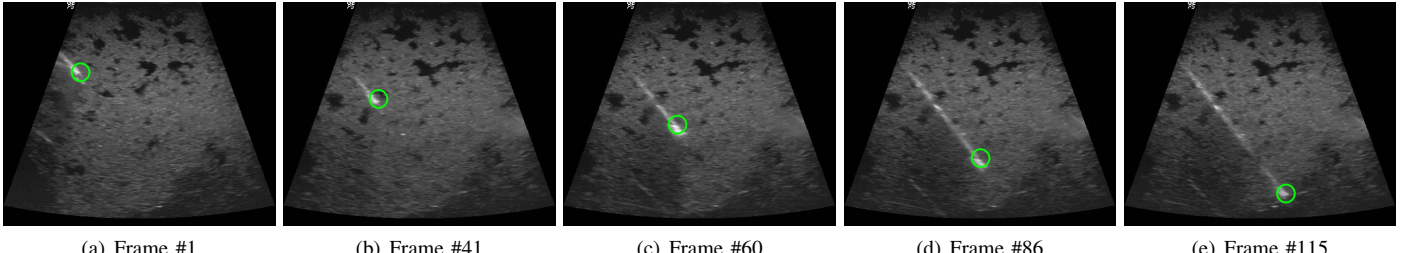


Fig. 2: Results of the proposed needle tip localization algorithm when time step (dt) equals 0.2 seconds.

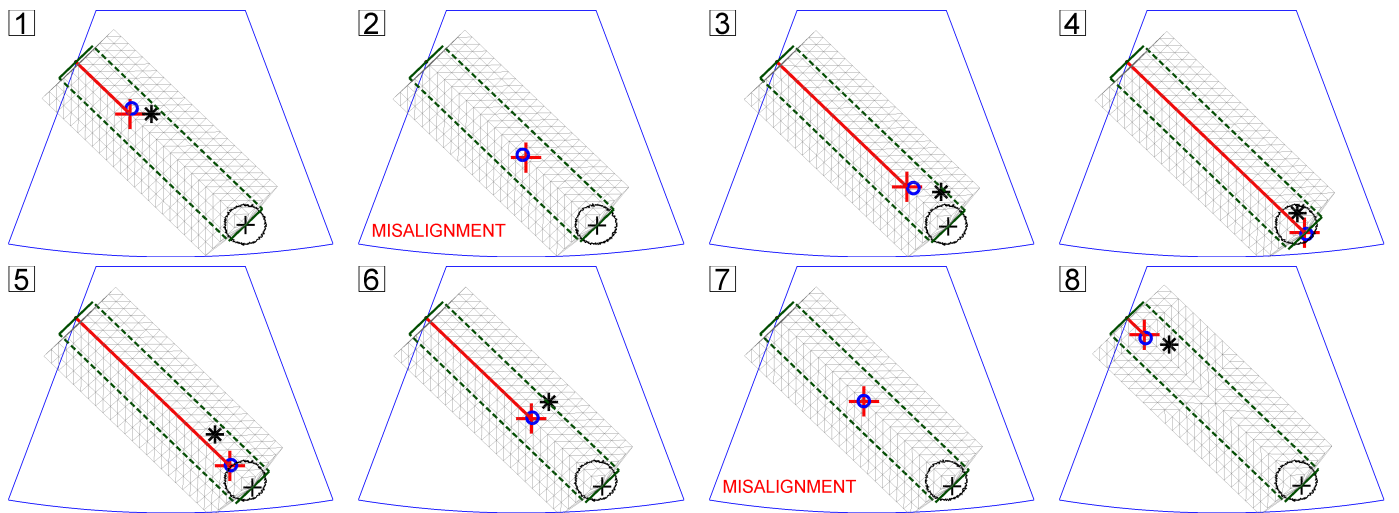


Fig. 3: Simulation snapshots of the needle tip tracking are shown. The needle insertion ROI is drawn with dashed lines. For this configuration 11×24 2D-nodes are created, the width of the meshes equals two times the needle insertion ROI. The tissue is not rigid. The circular region indicates suspicious region, and the '+' in the region indicates the target. The linear line in the needle insertion ROI indicates the needle, and the actual tip of the needle is shown using '+'. The estimated needle tip and the Kalman filter output are represented using '*' and 'o', respectively. Misalignment states are indicated by labels, and the needle is not visible. As it is shown with snapshots, the Kalman filter can estimate the position of the needle tip when it is not visible.

where

$$A = \begin{bmatrix} 1 & 0 & dt & 0 \\ 0 & 1 & 0 & dt \\ 0 & 0 & 1 & 0 \\ 0 & 0 & 0 & 1 \end{bmatrix} \quad \text{and} \quad H = \begin{bmatrix} 1 \\ 1 \\ 0 \\ 0 \end{bmatrix} \quad (1)$$

The process noise (w_k) and the measurement noise (v_k) are assumed to be zero mean Gaussian distributions with $\sim N(0, Q)$ and $\sim N(0, R)$ respectively. Q and R are the noise covariance and the measurement noise covariance matrices. These matrices are set manually and they are related to the Kalman filter performance. In order to evaluate the Kalman filter performance in realistic conditions and to obtain optimum values for the Q and R matrices, a simulation for the needle tip tracking is developed. The simulation is explained in detail in the following section.

IV. NEEDLE TIP TRACKING SIMULATION

The US images inherently are noisy. Developing new algorithms to improve needle tip localization can be slow

or complicated. Hence, a simulation platform is implemented to develop localization algorithms rapidly. Also, a simulation platform would be more effective to test different conditions of the system. For instance, the misalignment between the needle and the US image plane cannot be easily tested. The main purpose of the simulation is to improve the Kalman filter performance under different types of needle tip measurement noises. In order to simulate the needle tip tracking more realistically, tissue deformations and time-to-time image plane misalignments are incorporated. In Fig. 3, needle insertion and needle retraction are simulated. Misalignment cases of the needle and the tissue deformations are also illustrated. The needle tip estimation error versus time including the simulation steps shown in Fig. 3 are plotted in Fig. 4.

Input parameters for the simulation are: (i) The location of the target, (ii) The needle insertion angle, (iii) Width of the needle region of interest, (iv) The needle motion model, (v) The noise model of the needle tip measurement, (vi) The modulus of elasticity and the Poisson's ratio of the tissue, (vii) Applied force, and (viii) Simulation time step (dt). Output parameters for the simulation are: (i) Deformed mesh with respect to dt , and (ii) The error of the Kalman filter.

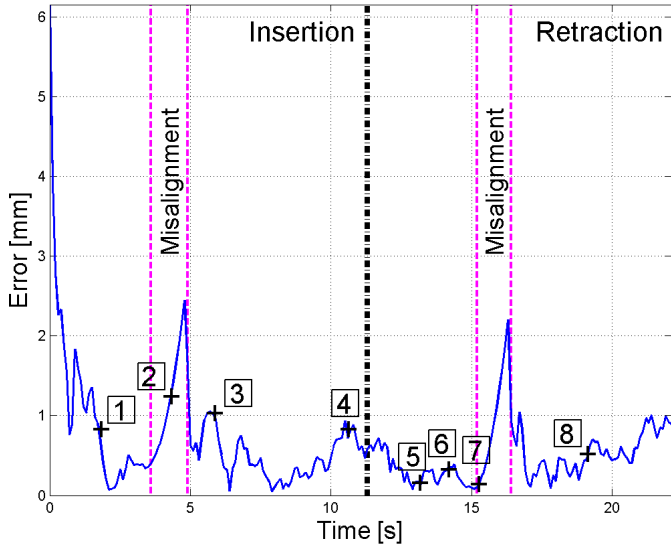


Fig. 4: Needle tip estimation error versus time. The error of each frame illustrated in Fig. 3 is marked with '+' and the corresponding frame number is indicated.

A virtual spring model was used to model the tissue deformation by [14]. In our simulations, the tissue assumed to be homogenous, and made of linearly elastic material [15]. While the needle is inserted with applied force ($F_{applied}$), the tissue resists the motion in the opposite direction. The reaction force causes the tissue's internal damping ($F_{damping}$) and stiffness ($F_{stiffness}$) forces. The total force applied to the needle tip to cut the tissue ($F_{cutting}$) is described by [16] [17]

$$F_{cutting} = F_{applied} - F_{stiffness} - F_{damping}$$

$$Ma_t = F_{applied} - Ku_t - Cv_t$$

where M, C and K are the mass, damping and stiffness matrices, respectively. a_t , v_t and u_t are the acceleration, velocity and position of the nodes at time t . The next position of the nodes (u_{t+1}) can be calculated as follows:

$$u_{(t+1)} = u_t + v_t dt + \frac{a_t dt^2}{2}$$

In our simulations, a rotated rectangular ROI is created according to the needle insertion angle and the target location (Fig. 3). The nodes are created using equal spaces and the nodes are triangulated using the Delaunay triangulations. In Figure 5, 2D 7x7 nodes are created and the figure shows the structural deformation while the needle is inserted into the tissue.

The Kalman filter performance is tested in realistic conditions using the simulation platform. Also, its performance with respect to different R and Q matrices is evaluated to obtain the optimum values. In real-time needle localization estimation, the noise is smoothed by obtaining the Kalman's R and Q matrices from the simulation.

V. BIN PACKING

In order to execute the proposed needle tip localization method in real time, its processing time should be decreased

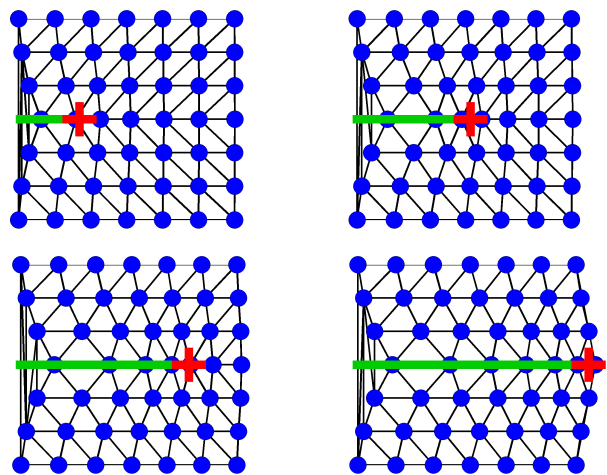


Fig. 5: Snapshots of the tissue deformation while the needle is inserted. 2D 7x7 nodes are created and shown with circles. The needle axis is shown using a linear line, and the '+' indicates its actual tip position.

significantly. The proposed needle localization algorithm is fairly complex, and consists of twelve main processing steps. During the localization, the frames are processed sequentially, since each processing step depends on the previous one's output. Also, partitioning the images into sub-images and processing these in parallel is not a good way to speed up the process, because the needle structure may not be detected, and combining these sub-images increases computational time. Hence, speeding up the processing time for a remarkable amount for single images is difficult. However, the frame sequences can be processed in parallel by applying the bin packing method to speed up the process.

The bin packing method divides the operations into equal time intervals and the processes are packed into bins. The processes in the bins are applied to different frames sequentially in separate threads. Each thread starts to process with a new incoming frame as the processes in the first bin are completed. The schematic representation of the sequential and bin packing methods are illustrated in Fig. 6. In this study, the processing time of the method's steps are measured (Table I), and accordingly the method is divided into four bins (P1, P2, P3, and P4) with respect to their processing times. It is assumed that the processing time of each bin is approximately equal to each other, $T/4$ at best. If a single image is processed at a time, in T time, the needle tip is localized in Frame #1 in thread #1.

However, if bin packing is used, the needle tip is localized in a thread, and that thread starts to work on the next frame. With bin packing, the needle tip is localized in four consecutive frames in $1.75T$ time at best, while four frames can be analyzed using a sequential processing method in $4T$ time.

A pipeline is a structure under which the execution of the instructions by a CPU is divided into several stages, with the operation to progress along the various units responsible for processing each stage. As a result, it is possible to start executing the next instruction without waiting for the execution

of the preceding one to be completed, so the program execution can be accelerated. The bin packing method reduces the processing time by 56% at best using CPU efficiently. This value was calculated by finding the difference between $4T$ and $1.75T$, then dividing the result of this subtraction by $4T$. If the proposed needle localization processes with the bin packing method, the needle tip can be localized in real-time without needing a GPU.

	Process	Process Time (ms)	Bin
#1 st Stage	Image Read	2.51 ± 0.41	(P1)
	Gabor Filter	0.92 ± 0.18	
	Median Filter	7.43 ± 1.22	
	Otsu Thresholding	0.42 ± 0.09	
	Parameter Tuning	1.98 ± 0.39	(P2)
	Morphological Opr. RANSAC Line Fitting	0.10 ± 0.02 3.99 ± 0.55	
#2 nd Stage	Gabor Filter	0.31 ± 0.05	(P3)
	Median Filter	7.25 ± 1.13	
	Otsu Thresholding	0.31 ± 0.06	
	Parameter Tuning	1.70 ± 0.21	(P4)
	Needle Tip Estimation	3.31 ± 0.34	
Overall Processing Time			35.01 ± 3.04

TABLE I: Processing time of each process in Fig. 1.

VI. EXPERIMENTS

A. Experimental Setup

1) *Biopsy Robot - OBR*: The robotic system that was used to insert needles is called OzU Biopsy Robot (OBR), and it has 5-DOF (see Fig. 7). It is designed to conduct biopsies on humans.

2) *US Machine*: The images were acquired using a LOGIQ P5 2D US machine (General Electric, USA), with a linear 2D US probe (11L, General Electric, USA). The acquired images were 640×480 pixels. The images were captured from the US machine with EURESYS PICOLA HD 3G frame grabber.

3) *Phantom*: Four different types of phantoms and distilled water were used during needle insertion experiments. These are distilled water (@ 25°C), distilled water and ethanol mixture (@ 25°C), gelatin-based, agar-based, and gelatin and agar mixture phantoms. These phantoms were prepared according to the recipes given in [13], [18]. In the experiments, 22 gauge biopsy needles were used.

4) *Execution Time*: The algorithm was implemented in C++ using the OpenCV library, and run on a 64-bit Window 7 workstation, which has an Intel Xeon E5-2620 CPU running at 2 GHz and 32 GB of RAM. The execution time of the proposed needle axis localization and needle tip estimation for a single image is 17.00 ± 2.03 ms and 12.95 ± 1.54 ms, respectively.

112 frames were used to measure the processing time of the sequential and the bin packing methods. The execution time of localizing the needle tip in a frame with sequential and the bin packing methods is 35.01 ± 3.04 ms, 13.28 ± 3.30 ms, respectively. Therefore, the bin packing method reduces the processing time by 56%.

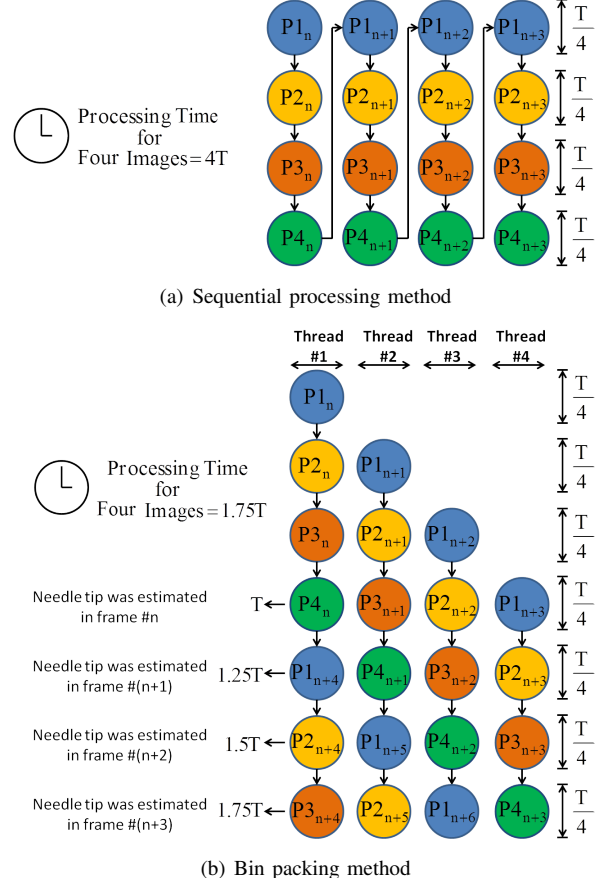


Fig. 6: Schematic representations of sequential and bin packing methods. Processing time of each bin ($T/4$) is assumed to be equal to each other. At the best case, the processing time of the localizing needle tip in four frames with (a) sequential and (b) bin packing methods are $4T$ and $1.75T$, respectively. Notice that processing time of the needle localization in the first frame is equal in two methods.

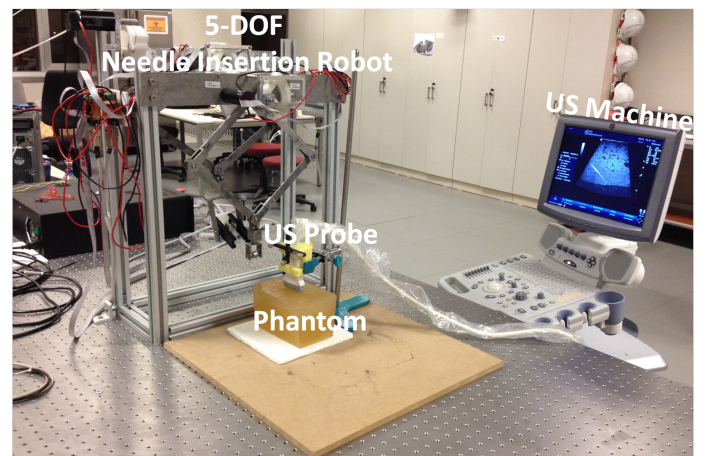


Fig. 7: View of 2D US guided 5-DOF robotic system for percutaneous needle procedures.

B. Needle Localization Results

1) Simulation Results: The needle tip tracking accuracy was initially evaluated with a simulation study. OBR inserts the needle with a PD controller, so in the simulation the needle tip reaches the target with the PD controller. In the simulation dt was set to 50 ms and the duration of the needle insertion and the retraction are assumed to be equal. This simulation was repeated 50 times and 11100 frames were evaluated. The parameters were tuned to get minimum and maximum error of the proposed tracking error. The minimum and maximum RMS error of the proposed tracking method in the simulations are 0.25 mm and 0.84 mm, respectively.

2) Experimental Results: The accuracy of the needle insertion angle estimation and the needle tip localization methods were evaluated using the OptiTrack optical motion capture system. 11.4 mm diameter optical markers were attached to the ultrasound probe and the needle. In order to find the needle tip position in 2D US image using motion capture, the system was calibrated with the proposed system in [19]. The needle was inserted to the agar-gelatin based phantom manually. After the needle was inserted, the angle value and the tip position were measured both by the optical tracking system and the proposed estimation method simultaneously.

54 2D single US images were used to evaluate the accuracy of the proposed insertion angle estimation. The error of the method is $1.95^\circ \pm 1.15^\circ$ (mean \pm standard deviation). 38 images were used to evaluate the accuracy of the needle tip localization. In order to find the error of the proposed method, the Euclidean distance between the actual needle tip location and the estimated needle tip location were calculated for each frame. The error of the proposed localization method is 1.22 ± 1.22 mm.

In this study, four different types of phantoms and a water medium were used to evaluate the algorithm capability to localize the needle axis and its tip in different contrast levels. Realistic phantoms were used specifically to prove that the proposed method works in a variety of US images with distinct backgrounds. 20 phantoms in total were used in the experiments. The needle was inserted into each phantom at least 30 times and approximately 3 US images were captured in each insertion. In total, 1417 single 2D US images from different types of phantoms were used to evaluate the algorithm. In all of the images, the needle trajectory and its tip were localized successfully. The algorithm was able to localize the biopsy needle axis and its tip in all of phantoms confirming the robustness of the method.

VII. ACKNOWLEDGMENT

This work was supported by the Scientific and Technical Research Council of Turkey (TUBITAK) under Grant No. 112E312.

- [2] G. Vrooijink, M. Abayazid, and S. Misra, "Real-time three-dimensional flexible needle tracking using two-dimensional ultrasound," in *Proceedings of the IEEE International Conference on Robotics and Automation (ICRA)*, no. 2, May 2013, pp. 1680–1685.
- [3] P. M. Novotny, J. A. Stoll, N. V. Vasilyev, P. J. del Nido, P. E. Dupont, and R. D. Howe, "Gpu based real-time instrument tracking with three dimensional ultrasound," in *Proceedings of the 9th international conference on Medical Image Computing and Computer-Assisted Intervention - Volume Part I*, 2006, pp. 58–65.
- [4] P. Chatelain, A. Krupa, and M. Marchal, "Real-time needle detection and tracking using a visually served 3d ultrasound probe," in *Proceedings of the IEEE International Conference on Robotics and Automation (ICRA)*, no. 2, May 2013, pp. 1668–1673.
- [5] K. Mathiassen, D. Dall Alba, R. Muradore, P. Fiorini, and O. Elle, "Real-time biopsy needle tip estimation in 2d ultrasound images," in *Proceedings of the IEEE International Conference on Robotics and Automation (ICRA)*, no. 2, May 2013, pp. 4348–4353.
- [6] A. Ayvaci, P. Yan, S. Xu, S. Soatto, and J. Kruecker, "Biopsy needle detection in transrectal ultrasound," *Computerized Medical Imaging and Graphics*, vol. 35, pp. 653 – 659, 2011.
- [7] M. Ding and A. Fenster, "A real-time biopsy needle segmentation technique using hough transform," *Medical Physics*, vol. 30, no. 8, pp. 2222–2233, 2003.
- [8] K. Cao, D. Mills, and K. Patwardhan, "Automated catheter detection in volumetric ultrasound," in *Biomedical Imaging (ISBI), 2013 IEEE 10th International Symposium on*, April 2013, pp. 37–40.
- [9] M. Renfrew, Z. Bai, and M. Cavusoglu, "Particle filter based active localization of target and needle in robotic image-guided intervention systems," in *Automation Science and Engineering (CASE), 2013 IEEE International Conference on*, Aug 2013, pp. 448–454.
- [10] T. K. Adebar and A. M. Okamura, "3d segmentation of curved needles using doppler ultrasound and vibration," in *Information Processing in Computer-Assisted Interventions*. Springer, 2013, pp. 61–70.
- [11] M. Fronheiser, S. Idriss, P. Wolf, and S. Smith, "Vibrating interventional device detection using real-time 3-d color doppler," *Ultrasonics, Ferroelectrics and Frequency Control, IEEE Transactions on*, 2008.
- [12] M. Kaya and O. Bebek, "Needle localization using gabor filtering in 2D ultrasound images," in *Proceedings of the IEEE International Conference on Robotics and Automation (ICRA)*, May 2014 2014.
- [13] ———, "Gabor filter based localization of needles in ultrasound guided robotic interventions," in *IEEE International Conference on Imaging Systems and Techniques (IST)*, October 2014.
- [14] Z. Yuan, Y. Zhang, J. Zhao, Y. Ding, C. Long, L. Xiong, D. Zhang, and G. Liang, "Real-time simulation for 3d tissue deformation with cuda based gpu computing," *Journal of Convergence Information Technology*, vol. 5, no. 4, pp. 109–119, 2010.
- [15] R. Alterovitz, K. Goldberg, J. Pouliot, R. Taschereau, and I.-C. Hsu, "Sensorless planning for medical needle insertion procedures," in *Intelligent Robots and Systems, 2003.(IROS 2003). Proceedings. 2003 IEEE/RSJ International Conference on*, vol. 4, 2003, pp. 3337–3343.
- [16] A. M. Okamura, C. Simone, and M. D. O'Leary, "Force modeling for needle insertion into soft tissue," *Biomedical Engineering. IEEE Transactions on*, vol. 51, no. 10, pp. 1707–1716, 2004.
- [17] R. Alterovitz and K. Goldberg, "Comparing algorithms for soft tissue deformation: accuracy metrics and benchmarks," *Rapport technique, UC Berkeley: Alpha Lab*, pp. 42–44, 2002.
- [18] ———, "A review of tissue substitutes for ultrasound imaging," *Ultrasound in Medicine and Biology*, vol. 36, no. 6, pp. 861 – 873, 2010.
- [19] A. Ahmad, C. Cavusoglu, and O. Bebek, "Calibration of 2D ultrasound in 3D space for robotic biopsies," in *International Conference on Advanced Robotics (ICAR)*, Istanbul, Turkey, 2015.

REFERENCES

- [1] K. Cleary, A. Melzer, V. Watson, G. Kronreif, and D. Stoianovici, "Interventional robotic systems: applications and technology state-of-the-art," *Minimally Invasive Therapy & Allied Technologies*, vol. 15, no. 2, pp. 101–113, 2006.